DRILLING AND CUTTING OF ALUMINUMS ALLOYS THIN SHEET OPTIMIZATION BY Nd:YAG LASER

Şef lucr. dr. ing. Ioan-Sorin LEOVEANU
Universitatea „Transilvania" din Braşov

Este absolvent al Universităţii „Transilvania" din Braşov, Facultatea de Tehnologia Construcţiilor de Maşini, Secţia utilajul şi tehnologia sudării. A efectuat stagiul la U. „Tractorul" din Braşov şi la I.P.T. Întorsura Buzăului, apoi a fost inginer proiectant la Institutul de Cercetare pentru Autovehicule şi Tractoare – Braşov, la departamentul punţi motoare directoare. Din 1988 este cadru didactic la Universitatea „Transilvania" din Braşov, la Catedra de Ingineria Materialelor şi Sudării. Este doctor inginer al Universităţii „Politehnica" din Bucureşti, din 2002. A contribuit la proiectarea punţilor motoare cu unghi mărit de virare pentru tractoare agricole şi industriale, la proiectarea şi omologarea structurilor de rezistenţă sudate pentru tractoare industriale şi agricole, la proiectarea unor noi tipuri de echipamente de buldozer si scarificator. A publicat manuale şi monografii pe plan local, central şi în colaborare cu universităţi din străinătate, precum şi articole în reviste şi în buletinele unor conferinţe de specialitate din ţară şi din străinătate.

Prof. dr. ing. Kim WON-TAE
Universitatea Cheongju, Republica Coreea

Este absolvent al Universităţii Naţionale din Seoul, departamentul de metalurgie, unde a urmat studiile de master absolvite în 1981 şi cele de doctorat absolvite în 1987. An fost asistent la Colegiul de Inginerie din Seoul şi până în anul 1991 a activat ca cercetator la Departamentul de Materiale al Universitătii Oxford. Este profesor de ştiinţe aplicate la Universitatea Cheongju şi conduce şi grupul de cercetare în domeniul materialelor ne-cristaline de la Universitatea Yonsei din Seoul. S-a specializat în domenii de vârf ale metalurgiei fizice, cum ar fi modelarea microstructurilor obţinute în urma solidificării rapide a materialelor, modelarea procesului de solidificare cu ajutorul metodei cîmpului fazelor ca şi în domeniul dezvoltării aliajelor amorfe (sticle metalice), modelarea fenomenului, estimarea şi caracterizarea proprietătilor structurilor amorfe astfel obţinute. A publicat numeroase lucrări ştiintifice în publicaţii de prestigiu.

REZUMAT. În lucrare se prezintă un model de calcul destinat analizei procesului de tăiere cu laser, model în care se ţine seama de parametrii proprii procesului de tăiere cu laser, parametrii caracterizaţi de modul de distribuţie a intensităţii generate de sursa laser, de procesele termice care guvernează topirea materialului ce se prelucrează ca şi de fenomenele hidrodinamice din materialul topit şi vaporizat şi din gazul de protecţie. Echilibrul local al acestor parametrii conduce la obţinerea geometriei frontului de tăiere şi la determinarea aspectului suprafeţei tăieturii obţinute . Datele astfel obţinute au fost comparate cu rezultate experimentale, iar corelaţia între modelul analizat şi cele experimentale s-a dovedit suficient de ridicată.

Cuvinte chele: model numeric, taiere cu laser, proces hidrodinamic, experiment.

ABSTRACT. In the paper is presented a numerical model of the laser cutting process where was taken into account the main parameters of the process that are the laser beam intensity distribution, the thermal phenomena controlling the melt parameters, the fluid, both cutting gas and melt hydrodynamics, and the local equilibrium of the geometry of the cutting front. The local equilibrium of these parameters gives the front cutting geometry and the geometry of the cutting surface obtained. In a second step, data provide by these simulations are compared with experiments and a good correlation is observed.

Key words: numerical model, laser cutting, hydrodynamic process, experiment.

1. INTRODUCTION

For many years, laser drilling and cutting technology has been used in industries because of its high accuracy and efficiency. In time it has been improved more pragmatically through experiences by industrial users. However full understanding of the process is not achieved up to now due to complicated interactions of several basic phenomena acting together, though a lot of works and experiments have been carried out, and entire description is still on a way of research. We can mention global work of Petring [1]. Kaplan [2] has undertaken a simpler complete description; however, no real closure condition is exposed. Concerning basic phenomenon studies, we can quote Schluz [3] who described thermal losses owing to heat diffusion in the sample. Cutting gases properties and dynamics have

been discussed in references [4] and [5]. Vicanek [6] highlighted hydrodynamic mechanisms, and the influence of gas jet onto melt layer.

Laser cutting can be viewed as a thermal issue. The laser beam either stay on the hole position or move with respect to the metal sheet. As the laser power is absorbed at the sample surface, its local temperature rises. As the temperature reaches the fusion temperature, melting starts to form liquid film with the geometry given by Marangoni convection. With heating further evaporation takes place on liquid film surfaces. This latter brings a force called recoil pressure and liquid/vapor interface starts to be formatted. In laser cutting and drilling, a high-pressure assistance gas is supplied into a co-axial direction to the laser beam. Argon gas is common in case of inert gas while nitrogen gas is frequently used in the Aluminum alloys. Combined with recoil pressure, it helps to dig the sample surface and creates the cutting kerf. The tangential component of the gas stream is responsible for the vertical ejection of the molten material because of the shearing forces acting on the melt. The aim of this article is to give a mathematical model description of the laser kerf formation and drilling process. The process of laser drilling can be schematically presented in figures 1a and 1b. Finally, we will see that numerical calculation results catch basic features of laser drilling process and in reasonable agreement with experimental data. This model provides maximum drilling depth achievable for a given material properties and input parameters such as laser power, initial gas pressure, cutting speed and focal point position.

The starting point of this work needs to describe the local physical equilibrium of each cell of the drilling front.

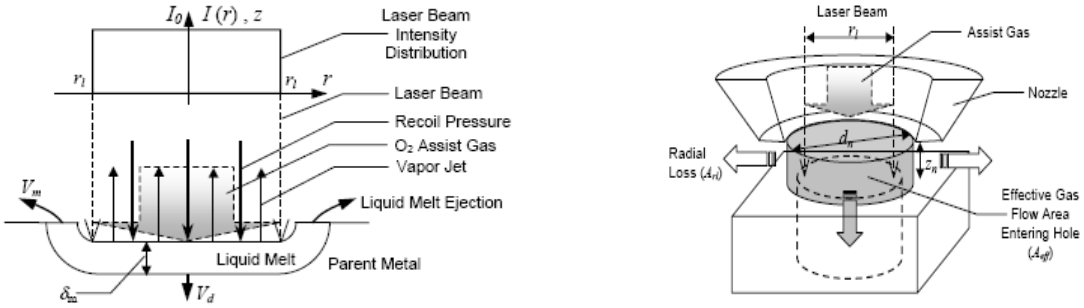

Fig. 1. The presentation of laser drilling process based on numerical modeling studied in the paper.
a – schematic diagram of physical model; *b* – schematic gas flow entering the hole and area of radial loss flow.

2. GOVERNING EQUATIONS

During laser drilling process, the absorbed energy heats the specimen surface above its melting point to the vaporization temperature and then the liquid melt is ejected by recoil pressure and assistant gas if necessary. The vapor pressure builds an opposite pressure, exerting a force on the melt surface and expels the melt from the surface of the hole.

The initial heating and pressure build-up stage can be described by a combination of following governing equations: conservation of mass equation (1), Navier Stokes equations for momentum equation (2), heat flow in fluid equation (3), and species transfer equations (4)-(5):

$$\frac{\partial \rho}{\partial t} + \nabla\left(\rho \cdot \vec{V}\right) = 0 \tag{1}$$

$$\frac{\partial}{\partial t}\left(\rho \cdot \vec{V}\right) + \nabla\left(\rho \cdot \vec{V} \times \vec{V}\right) = -\nabla p + \rho \cdot \vec{g} \tag{2}$$

$$\frac{\partial}{\partial t}\left(\rho \cdot E\right) + \nabla\left(\rho \cdot E + p\right) \cdot \vec{V} = \nabla\left(\lambda \cdot \nabla T\right) \tag{3}$$

$$\frac{\partial}{\partial t}\left(\rho_i \cdot C_i\right) + \nabla\left(\rho_i \cdot \vec{V} \cdot C_i\right) = 0 \tag{4}$$

$$\sum_{i}^{ns+1}\left(\rho_i \cdot C_i\right) = \rho \tag{5}$$

where ρ is the density of gas phase, C_i the concentrations of the chemical elements, ρ_i the density of vapors and shielded gas in the area of alloyed element expulsed, $\vec{V}$ the velocity of the components, p the pressure, E the enthalpy of the gases, λ the heat conductivity of the gases system, T the temperature.

The equations (1)-(3) are used to modelling the shielded gas movement and their results are served as a first approximation of the initial conditions on the surface of solid part (the melted film creation). The sketch of this first step of numerical simulation process can be seen in figure 2.

Laser geometry modelling. Stainless steel, alloy steel and tool steel etc. can be cut and drilled very well using CO_2 lasers. However, CO_2 laser is not suitable for cutting Cu and Al material due to their

high reflectivity and high thermal conductivity. Nd:YAG lasers which have shorter wavelength than CO_2 laser can be used for Cu and Al materials. In general, higher average laser power is required for cutting metal than nonmetals because the former has higher reflectivity and thermal conductivity. In this simulation, nitrogen gas was used as the shielded gas but the oxygen assisted cutting was not taken into consideration even though it is more commonly used in industry.

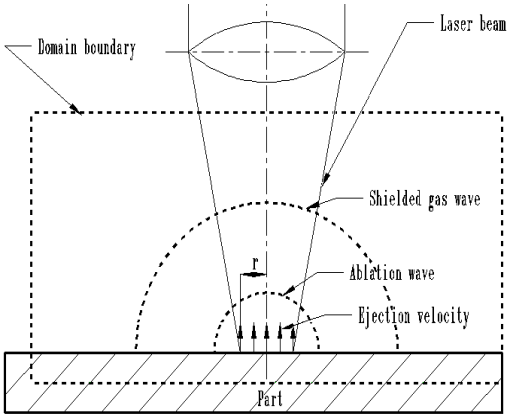

Fig. 2. The sketch of the analyzed gaze domain in the initial step of numerical process.

The laser spot intensity can be expressed as follows:

$$I_{(x,y)} = I_0 \cdot \exp\left(-\frac{x^2+y^2}{r^2}\right) \quad (6)$$

where x, y are the distance from the center (0, 0) of the laser beam in the x, y direction, I_0 is the laser intensity at (0, 0). The concept of M^2 is useful for description of actual propagation of laser beams. M^2 is a beam quality index that measures the difference between an actual beam and the Gaussian beam. In order to find out the M^2 of a laser system, we need first measure the spot size along the laser optical axis. The cut edge method, based on the geometrical characteristics as in figure 3 is used to establish the DOF distance:

$$D_{\min} = \frac{4 \cdot f \cdot M^2 \cdot \lambda}{\pi \cdot D_L}, \quad \theta_{Gaussian} = \frac{\lambda}{\pi \cdot D_0} \quad (7)\text{-}(8)$$

$$\theta_{act} = \frac{M^2 \cdot \lambda}{\pi \cdot D_0}, \quad DOF = \pm 0.08 \cdot \pi \frac{D_{\min}^2}{M^2 \cdot \lambda} \quad (9)\text{-}(10)$$

where D_L is the laser beam size when it propagates to the front side of the focus objective lens, f is the focus length; D_{min} is the minimum beam diameter that can be achieved; θ_{act} is the real beam divergence.

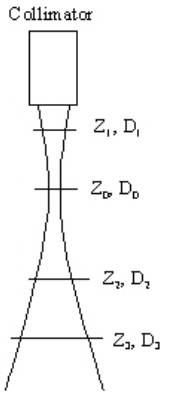

Fig. 3. The laser spot characteristics for DOF established.

For a Gaussian beam with beam radius r and for a material with absorption $A = 1 - R$, where R is the reflectivity, we have:

$$I(x,y,z,t) = (1-R) \cdot I_0 \cdot \exp(-a \cdot z) \cdot \exp\left(-\frac{x^2+y^2}{r^2}\right) \quad (11)$$

and the using the 1D approximation of the temperature in the drilled finite volumes the following expressions:

$$\text{if } 0 < t < t_p$$

$$T(z,t) - T_0 = 2\frac{I_0}{\lambda}\sqrt{t \cdot a} \cdot ierfc\left(\frac{z}{2\sqrt{t \cdot a}}\right) \quad (12)$$

where λ is the heat conductivity, I_0 is the absorbed laser intensity, t is time, t_p is the pulse duration, z is distance from the top surface. T_0 is the initial temperature, *ierfc(u)* define the complementary error function.

$$ierfc(u) = \frac{\exp(-u^2)}{\sqrt{\pi}} - u(1 - erf(u))$$

The material will start to cool down if the power is turned off at $t = t_p$. This cooling down process for pulse paused period ($t > t_p$) is computed with the following equation:

$$T(z,t) - T_0 = 2\frac{I_0}{\lambda}\left[ierfc\left(\frac{z}{2\sqrt{t \cdot a}}\right)\sqrt{t \cdot a} - ierfc\left(\frac{z}{2\sqrt{a \cdot (t - t_p)}}\right)\sqrt{(t - t_p) \cdot a}\right] \quad (13)$$

With the above two equations can be calculated the 1D heat conduction into a semi-infinite body with a single pulse, location fixed and constant amplitude heat source. In this temperature distribution calculation, the vaporization and melting phenomena was not considered.

In order to account for these phenomena, the latent heats of melting and vaporization will be included inside the control volume in the program of modeling phenomenon. Using energy balance relationship, i.e., increase of stored energy in a volume of material = energy input + + energy generation in this volume - energy output, we can derive a general differential form of three dimensional heat conduction equation. In short:

$$E_{in} + E_g - E_{out} = \Delta E_{st} \tag{14}$$

If material is homogeneous and uniform in property, the governing equation of heat flow in the drilling area has the expression:

$$\frac{\partial^2 T}{\partial x^2} + \frac{\partial^2 T}{\partial y^2} + \frac{\partial^2 T}{\partial z^2} + \frac{1}{\lambda}\frac{dq_L}{dt} = \frac{1}{a}\frac{\partial T}{\partial t} \tag{15}$$

where a is the thermal diffusivity and the term $\mathrm{d}q_L / \mathrm{d}t$ corresponds to the heat generation in control volume, accounting for the melting or vaporization processes.

The temperature approximations in the melting process considerations for the laser spot heated area. a) Case when both temperatures are within solidus and liquidus temperatures at moment $\Delta t = t_2 - t_1$, b and c) when only one temperature is outside the melting range [23, 24].

The latent heat of melting generated inside the control volume, Δq_L is expressed as follow with a variation of liquid fraction f_L during a time step, the latent heat of melting of the control volume material Q_L, control volume V_i and density ρ, and liquid fraction can be expressed as a funtion of temperature T with solidus and liquidus temperatures T_S and T_L, respectively.

$$\Delta q_L = \rho \cdot c_v \cdot V_i \cdot \Delta T = \rho \cdot Q_L \cdot V_i \cdot \Delta f_L$$

$$f_L = \frac{T - T_S}{T_L - T_S} = 1 - f_S$$

In order to account for the melting behavior, temperature $T_2^{'}$ calculated from the equations (12) or (13) in the heated zone by laser spot at time t_2 should be corrected to a new temperature T_2 at time t_2. In this analysis, only the cases presented in figure 4 were considered, which results in following expressions [23]:

For case a):

$$E_i^{II} = \int_{t_1}^{t_2} \rho \cdot c_v \frac{\partial T}{\partial t} \cdot \mathrm{d}t - \Delta q_L =$$

$$= \int_{T_1}^{T_2} \rho \cdot c_v \cdot \mathrm{d}T + \int_{T_1}^{T_2} \rho \cdot Q_L \frac{\partial f_L}{\partial T} \cdot \mathrm{d}T$$

$$E_i^I = \int_{t_1}^{t_2} \rho \cdot c_v \frac{\partial T}{\partial t} \mathrm{d}t = \int_{T_1}^{T_2^{'}} \rho \cdot c_v \cdot \mathrm{d}T$$

$$\int_{T_1}^{T_2} \rho \cdot c_v \cdot \mathrm{d}T + \int_{T_1}^{T_2} \rho \cdot Q_L \frac{\partial f_L}{\partial T} \cdot \mathrm{d}T = \int_{T_1}^{T_2^{'}} \rho \cdot c_v \cdot \mathrm{d}T$$

For case b)

$$\int_{T_S}^{T_2} \rho \cdot c_v \cdot \mathrm{d}T + \int_{T_S}^{T_2} \rho \cdot Q_L \frac{\partial f_L}{\partial T} \cdot \mathrm{d}T = \int_{T_1}^{T_2^{'}} \rho \cdot c_v \cdot \mathrm{d}T$$

For case c)

$$\int_{T_L}^{T_2} \rho \cdot c_v \cdot \mathrm{d}T + \int_{T_L}^{T_2} \rho \cdot Q_L \frac{\partial f_L}{\partial T} \cdot \mathrm{d}T = \int_{T_1}^{T_2^{'}} \rho \cdot c_v \cdot \mathrm{d}T$$

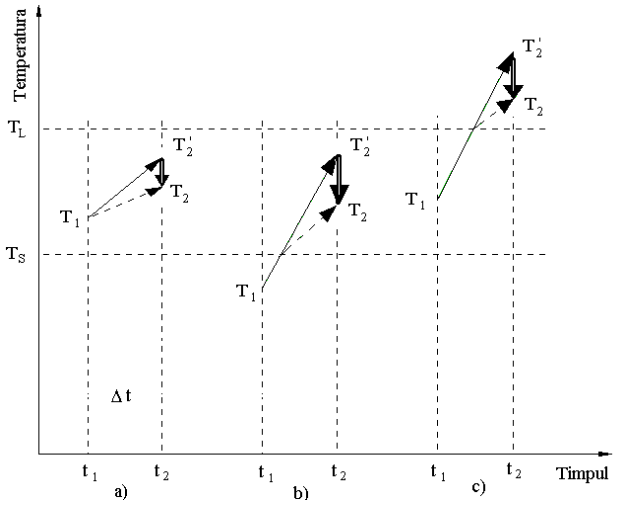

Fig. 4. The temperature approximations in the melting processes considerations for the laser spot heated area.

Governing equations at fluid flow area. The momentum and mass conservation equations in fluid flow area for the melted material can be expressed as follows:

$$\frac{\partial \vec{v}}{\partial t} + \mathrm{Re} \cdot (grad\,\vec{v}) \cdot \vec{v} = -(grad\,\vec{p}) + \Delta \vec{v} \tag{16}$$

$$(div\,\vec{v}) = 0 \tag{17}$$

The system of equations was solved used MAC method and the results are done for an example. An example of gas phase model solutions for a train of pulses with P = 4 kW and 5 μs are shown in figure 5. These information are used in determination of the boundary conditions on the free surface of the melted area and on the surface of the part. The 2D free surfaces model equations used in this program do not consider transversal stresses. The pressure and speed on the

surface was considered to be equal to those of the gases on the interfaces between liquid and gases [24, 22].

$$-p_{visc}+2\mu\frac{\partial u}{\partial x}n_x^2+ +2\mu\left(\frac{\partial u}{\partial y}+\frac{\partial v}{\partial x}\right)\cdot n_x n_y+2\mu\frac{\partial v}{\partial y}n_y^2=-p_{gaz} \quad (18a)$$

$$2\mu n_x n_y\left(\frac{\partial u}{\partial x}-\frac{\partial v}{\partial y}\right)+ +\mu\left(\frac{\partial u}{\partial y}+\frac{\partial v}{\partial x}\right)\cdot\left(n_y^2-n_x^2\right)=0 \quad (18b)$$

After melting and vaporization on melted surfaces, the model of gases is modified by usin theg following equations [26]:

$$p_{reac}=\frac{A\cdot B_0}{\sqrt{T_S}}\cdot\exp\left(\frac{-M_a\cdot L_v}{N_A\cdot k_B\cdot T_S}\right) \quad (19)$$

$$p_{reac}=\rho\cdot V_z^2 \quad (20)$$

$$J_V=\frac{p_{reac}}{V_z} \quad (21)$$

where A is Anisimov material coefficient [3], B the vaporization constant, M_a the molecular mass, L the latent heat of vaporization, N_A the Avogadro number, K_B the Boltzmann constant, T_S the temperature of the liquid surface, p_{rec} the recoil pressure of vapors, V_z speed of vapors, J_V vapor's expulsed fluxes. The temperature T_S used for p_{rec} estimation was established with the thin plate solution used for solving the system (1)-(5) and establish the beginning hole generation. The geometrical model grid size was 0.15 mm in all simulations.

3. EXAMPLES OF NUMERICAL CALCULATION

An example of numerical calculations for the melting and ablation process at the surface of drilled hole, obtained after the first train of laser pulse, is given in figure 7.

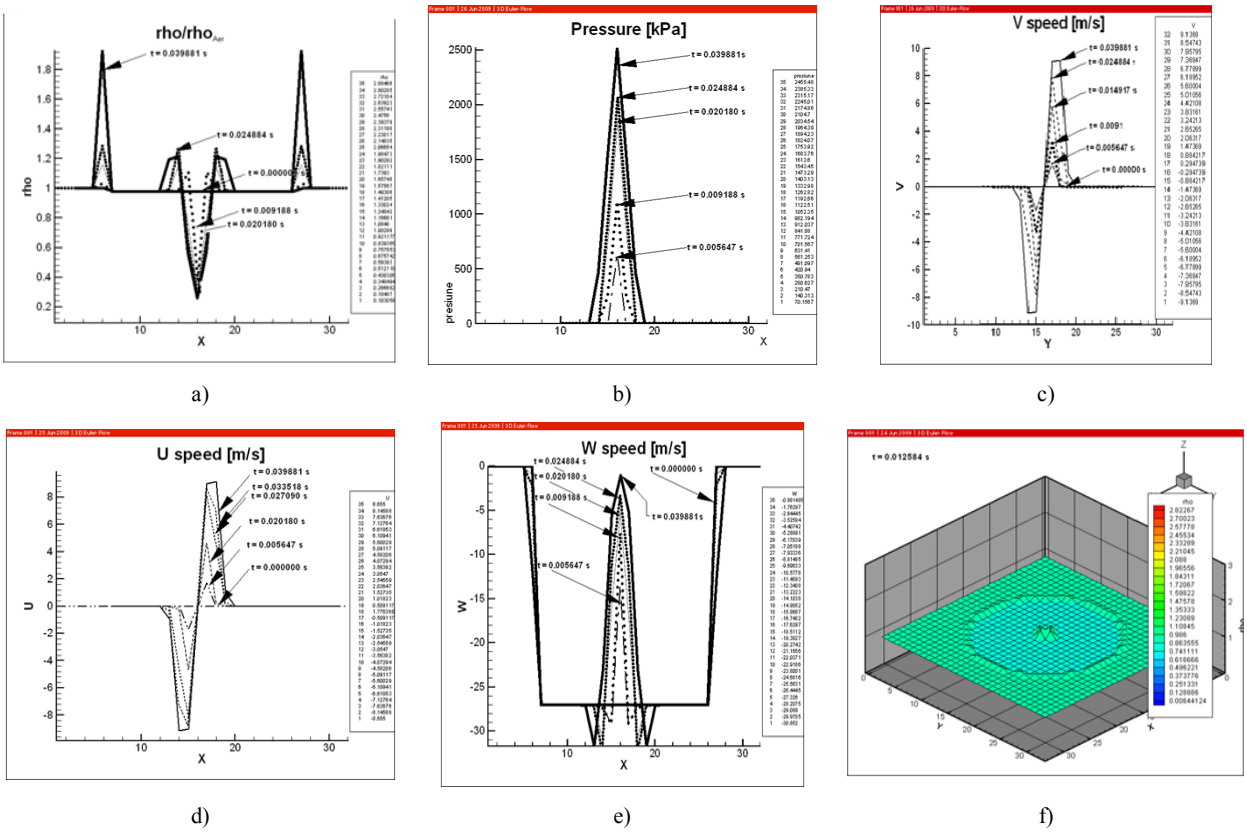

Fig. 5. The gases phase model solutions used in determination of the boundary conditions for melted pool calculation: *a* – the density of the Nitrogen gas during the heat laser pulses packet; *b* – the pressure of the expanded gas during the laser pulses packet; *c* – the speed on *Oy* direction of the expanded gas; *d* – the speed on *Ox* direction of the expanded gas; *e* – the speed on *Oz* direction during the expanded gas; *f* – the aspect of gas expanded fronts.

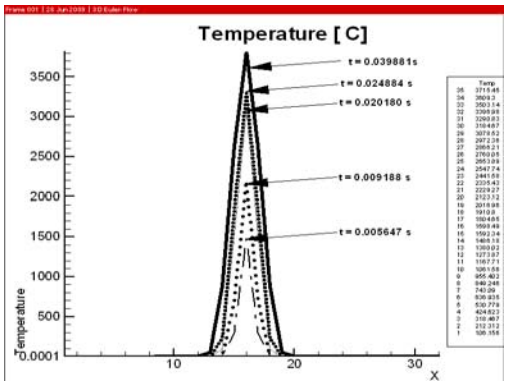

Fig. 6. The evolution of the temperature distribution in the gas near the impact of laser beam.

Table 1. **Physical properties of Al-3wt%Cu used in calculations**

Parameter	Measure Unit	Value
Solidus temperature, T_S	[^oK]	877,3
Liquidus temperature T_L	[^oK]	925,2
Thermal conductivity of liquid λ_L	[W m-1$^oK^{-1}$]	90
Thermal conductivity of solid λ_S	[W m-1 $^oK^{-1}$]	210
Specific heat C_p	[J Kg-1 $^oK^{-1}$]	900
Latent heat of melting L_t	[J kg^{-1}]	3.95 105
Coeff. Of thermal expansion, β	[$^oK^{-1}$]	2.5 10-5
Density, ρ	[kg m^{-3}]	2730
Heat of evaporation of Al	[J kg^{-1}]	1.078×10^7
Focal length of lens	[m]	0.16

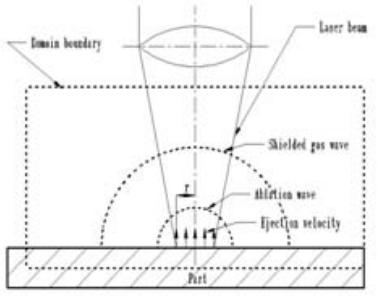

a)

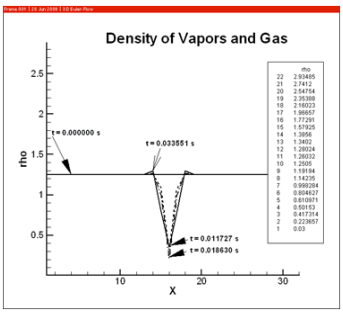

b)

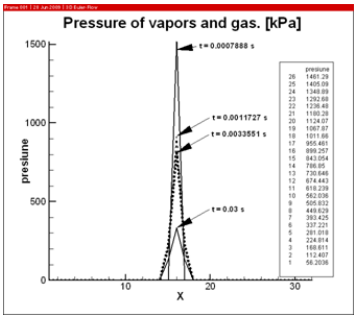

c)

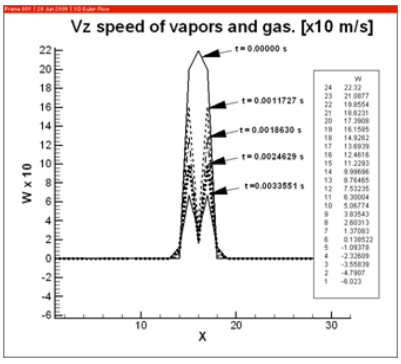

d)

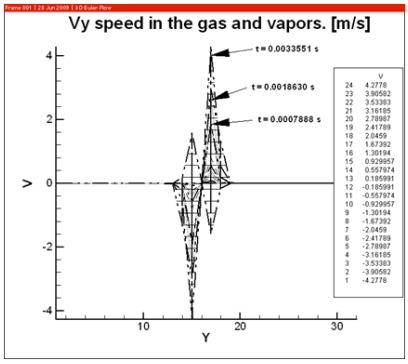

e)

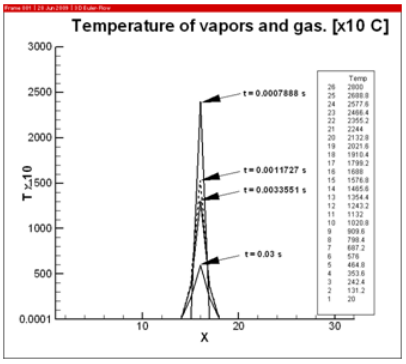

f)

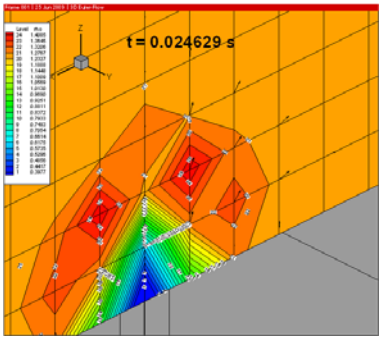

g)

Fig. 7. The evolution of gases parameters in the vaporization and ablation process during hole drilling process:
a – the domain geometry and front of waves position; *b* – the density of gazes at the boundary of the kerf and part surface; *c* – the pressure variation in the gazes phase; *d* – the speed on vertical direction; *e* – the speed on *Oy* direction; *f* – the temperature variation in the drilling area; *g* – density variation at 0,0025 s after process beginning.

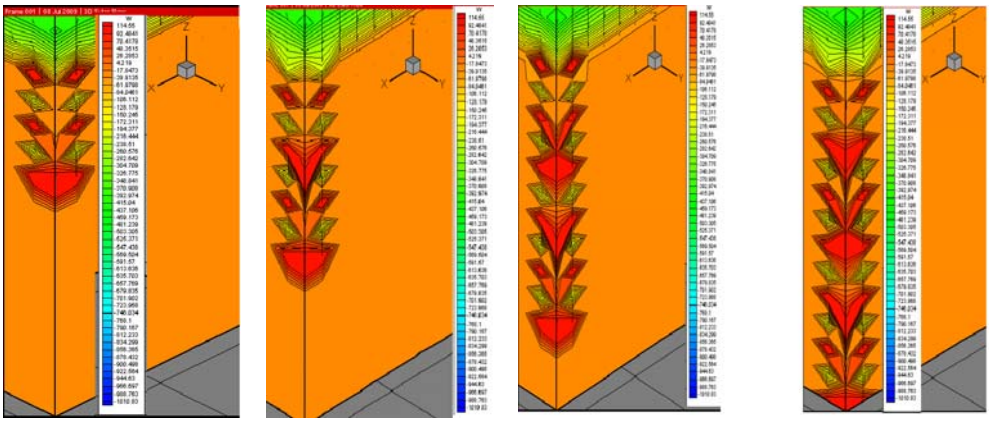

a) b) c) d)

Fig. 8. The drilling speed variation during the technological process using three pulses of each 1,5 ns and $I_0 = 4$ kW, I_1=1.25 kW and $I_2 = 500$ W:
a – the first 3 pulses of 1,5 ns; *b* – the second train of 3 pulses; *c* – the 3th train of 3 pulses; *d* – the 4th train of 3 pulses.

The current model deals with the control of liquid and vapors volume in the drilled area. The important issue is to keep a constant liquid volume by monitoring the pulse power and the delay between pulse trains.

Figure 8 shows some examples of drilling process simulation, performed for Al-3wt%Cu alloy with N_2 protection gas. The physical properties of the alloy used in the calculation are listed in Table 1. Numerical simulations were performed for drilling a hole of radius of 0.3505 mm in Al-wt3%Cu alloy. Also simulation was performed for electrolytic Cu thin sheet to drill holes of radius ranging from 0.35 mm to 1.2 mm, even though the results are not shown here due to page limit. Through the simulations it was found that the gas speed and pressure variation on the section of the hole drilled by laser are also important factors affecting surfaces geometry, which is in line with current practice.

3. SUMMARY

We developed a model accounting for most aspects of laser drilling and cutting process, which is a succession of several steps. The modeling process consisted of several stages, solving the Euler system of equations, the heat flow and melting and vaporization equations and the Navier-Stokes system of equations. The numerical code to solve these equations was developed using Microsoft Visual C/C++ and the solutions were implemented in the AMerican TEChnology post-processor, TechPlot version 8.0. The Euler system of equations was solved using TVD scheme with boundary conditions and CFD type Van Leer and MCD scheme of LeVeque. The Heat and Fluid Flow problems were solved using Volume Finite Method in version Marker And Cell for free boundary Navier Stokes problem.

Comparing with classical technology, relying on mainly trial and error, the numerical simulation was found to be very useful to design processing condition for drilling holes with very small diameter in alloys or materials, which can save time and cost. The numerical code and algorithms presented here is useful to understand the effect of each process variables and can be applied for process optimization. Finally the modeling will help to increase the laser drilling and cutting application area.

BIBLIOGRAPHY

[1] **Petring D.** *Anwendungsorientierte Modellierung des Laserstrahlschneidens zur rechnergestüzten Prozessoptimierung.* Verlag Shaker, Aachen, 1995.ISBN 3-8265-043-3X.

[2] **Kaplan A.** *An analytical model of metal cutting with a laser beam.* J. Appl. Phys. 79 (5), 1996

[3] **Schulz W., Becker D., Franke J., Kemmerling R., Herziger G.** *Heat conduction losses in laser cutting of metals*.J. Phys. D : Appl. Phys. 26, 1993, 1357-1363.

[4] **Man H.C., Duan J., Yue T.M.** *Dynamic characteristics of gas jets from subsonic and supersonic nozzles for high pressure gas laser cutting*. Elsevier Science B.V, 1999.

[5] **Fierret J., Thierry M.J., Ward B.A.** *Overview of flow dynamics in gas-assisted laser cutting*. *SPIE* , Vol 801, 1987, High Power Lasers, pp 243-250

[6] **Vicanek M., Simon G.** *Momentum and heat transfer of an inert gas jet to the melt in laser cutting*. J. Phys. D : Appl. Phys. 20, 1987, 1191-1196.

[7] **Fabbro R., Chouf K.** *Dynamical description of keyhole in deep penetration laser welding*. J. of Laser Appl. 2000, 12(4), pp 142-148

[8] **Oates W. R.,** editor, *Welding Handbook*, Materials and Applications, pt. 1, vol. 3, 8th ed., American Welding Society, Miami, Florida, 121-162, 1996.
[9] **Gaines L., Cuenca R., Stodolsky F., Wu S.**, *Analysis of the Potential for New Automotive Uses of Wrought Magnesium*, Argonne National Laboratory, Center for Transportation Research, ANL-ESD-35, Argonne, IL, February 1996.
[10] **Baeslack W. A., Savage S. J., Froes F. H.,** *J. Mater. Sci. Let*., 1986, vol. 5, pp. 935-9.
[11] **Chen G., Roth G., Maisenhalde F.R,** *Laser und Opto-elektronik*, 1993, vol. 25, pp. 43-7.
[12] **H. Haferkamp, F. Von Alvensleben, I. Burmester, and M. Niemeyer,** *Proc. ICALEO 97*, Laser Institute of America, Orlando, FL, 1997.
[13] **Housh S, Mikucki B., Stevenson A.**, *Properties of Magnesium Alloys in Metals Handbook,* 10th Edition, Volume 2, *Properties and Selection: Nonferrous Alloys and Special-Purpose Materials*, ASM International, Materials Park, OH.
[14] **Leong, K.H., Sabo K.R. Sanders, P.G., Spawr W.J.** *Laser Beam Welding of Aluminum Alloys.* SPIE Proceedings, Lasers as Tools for Manufacturing II. Vol. 2993:(1997).
[15] **Toulokian, Y.S., Powell, R.W., Ho, C.Y. And Nicolaou, M.C.** *Thermal Conductivity Metallic Elements and Alloys*, *Thermophysical Properties of Matter*, Vol. 1, New York: IFI/Plenum, 1970.
[16] **Lida T., Guthrie R. I. L.** *The Physical Properties of Liquid Metals*, Clarendon Press, Oxford, 1993.
[17] **Nonhof C. J.**, *Material processing with Nd-lasers*. Electrochemical Publications, Ayr, Scotland, 1988.
[18] **Leong K. H., Geyer H. K., Sabo K. R., Sanders P. G.**: *J. Laser Appl*.,9, 227-232.
[19] **Leong K. H., Sabo K. R., Sanders P. G., Spawr W. J.** *Laser Beam Welding of Aluminum Alloys*, SPIE Proceedings Vol. 2993 Lasers as Tools for Manufacturing II, 1997.
[20] **Forsythe W. E.**: *Smithsonian Physical Tables*, 9th ed., Smithsonian Institution, Washington D.C., 1959.
[21] **Kim J.-D., Katayama S., Mizutani M., Takemoto T.** *Rev. Laser Eng.,* 1996, vol. 24, pp. 996-1005.
[22] **Leoveanu I.S.** *Studies of the effect of Laser beam mode considerate by numerical simulation of welding performance for micro welding of thin Aluminum sheet by Nd:YAG Laser*. www.agir.ro/buletine/432.pdf, Buletinul AGIR, 2009.
[23] **Leoveanu I.S., Zgură Gh.**, *Modelling the Heat and Fluid Flow in the Welded Pool from High Power Arc Sources.* Advanced Welding and Micro Joining Packaging for the 21st Century. Series Materials Science Forum Vols. 580-582. Ed, ttp 2008. doi:10.4028/0-87849-383-2.443
[24] **Hong C. P., Umeda T., Kimura Y.**, *Metall Trans*., vol 15B.
[25] **Leoveanu I. S. Tierean, M. H.**. *Metode numerice avansate. Aplicaţii în modelarea metalelor*. Ed. Universitatii Transilvania din Braşov, 2009.
[26] **Vizman D., Cristea A., Sofonea V..** *Metode numerice avansate*. Ed. Eurobit. Timişoara, 2008.
[27] **Rai R., Kelly S. M. Martukanitz, R. P., Debroy T..** *A convective heat-transfer model for partial and full penetration keyhole mode laser welding of a structural steel*. Metal. And Mat. Trans. 2007.